

## Enhanced spin injection and magnetoconductance by controllable Rashba coupling in a ferromagnet/two-dimensional electron gas structure

This article has been downloaded from IOPscience. Please scroll down to see the full text article.

2003 J. Phys.: Condens. Matter 15 L31

(<http://iopscience.iop.org/0953-8984/15/2/105>)

View [the table of contents for this issue](#), or go to the [journal homepage](#) for more

Download details:

IP Address: 171.66.16.119

The article was downloaded on 19/05/2010 at 06:26

Please note that [terms and conditions apply](#).

## LETTER TO THE EDITOR

## Enhanced spin injection and magnetoconductance by controllable Rashba coupling in a ferromagnet/two-dimensional electron gas structure

Y Jiang<sup>1,2</sup> and M B A Jalil<sup>1</sup>

<sup>1</sup> Information Storage Materials Laboratory, Department of Electrical and Computer Engineering, National University of Singapore, 117576, Singapore

<sup>2</sup> Department of Material Science, Tohoku University, Sendai 980-8579, Japan

Received 13 November 2002

Published 6 January 2003

Online at [stacks.iop.org/JPhysCM/15/L31](http://stacks.iop.org/JPhysCM/15/L31)

### Abstract

In this letter, a new hybrid structure, which comprises of a ferromagnet (FM) deposited on a two-dimensional electron gas (2DEG), is proposed. We present numerical calculations of the ballistic spin-dependent transport properties of the structure in the presence of spin–orbit coupling as described by the Rashba Hamiltonian. It is shown that the gate electrode on top of the structure can be used to control the Rashba coupling and hence the spin injection in the 2DEG. For the typical InAs system assumed in our numerical calculations, the spin polarization in the 2DEG reaches a ratio of up to  $\sim 90\%$ . The structure is also predicted to show magnetoconductance behaviour upon switching the magnetization direction of the FM stripe. The large spin polarization and MC of the proposed structure demonstrate the potential of the device as a spin injector in spin-logic devices as well as a magnetic sensor with ultra-high density storage.

There exists a growing interest in the spin injection and manipulation of spin current in hybrid ferromagnet (FM)–semiconductor nanostructures, since the proposal by Datta and Das [1] of a spin-polarized field transistor, in which the spin precession can be controlled by an external electric field via spin–orbit or Rashba coupling [2]. It has been pointed out that a spin transistor must satisfy at least three conditions [3]:

- (i) long spin-relaxation time in a semiconductor,
- (ii) gate voltage control of the spin–orbit coupling and
- (iii) high spin-injection coefficient.

The first and second requirements have already been preliminarily established [4, 5]. As for the third requirement, many approaches, such as ohmic injection [6], tunnelling injection [3, 7] and ballistic electron injection [8], have been developed [9]. However, in all cases, the

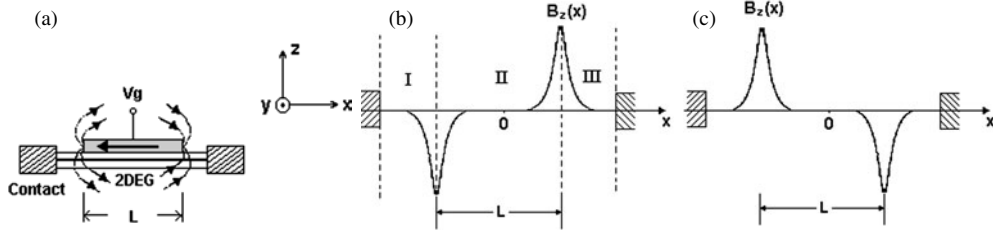


**Figure 1.** (a) Schematic overview of the device. (b) Perpendicular component of the magnetic field in the 2DEG corresponding to (a). (c) Perpendicular component of the magnetic field in the 2DEG when the magnetization of the FM stripe points towards the  $x$ -axis direction.

measured spin-polarization ratio was very small, and such low efficiency was attributed to the conductance mismatch between FM and semiconductor [10]. An alternative route is in using a ferromagnetic semiconductor or dilute-magnetic semiconductor for spin injection into the semiconductor [11], but their low Curie temperature preclude their usage in room temperature devices [3]. In this paper, we propose a new device comprising of an inverted two-dimensional electron gas (2DEG) heterostructure, on the top of which an FM is deposited. In this structure, the spin injection in the 2DEG comes from the Rashba spin splitting just as in the spin transistor of Datta and Das, but the spin polarization of current is induced by the inhomogeneous fringe magnetic field of the FM stripe, rather than passing it through the FM. Thus in the structure, the spin injection will not be frustrated by the mismatch of the conductances between the FM and semiconductor. By performing realistic numerical calculations, we show that the combined effect of the gate electrode on the top of the device and the fringe magnetic field from the FM stripe is sufficiently strong to induce a large spin polarization ( $\sim 95\%$ ) of current in the 2DEG. Additionally, the proposed structure exhibits a large magnetoconductance (MC) ratio. We show that its conductance is significantly changed upon the reversal of the magnetization of the FM stripe.

Figure 1(a) gives a schematic overview of the device, in which a metallic FM stripe of width  $L$  is deposited on a 2DEG heterostructure. The in-plane magnetization of the FM layers produces an out-of-plane fringe field at both ends. The fringe field constitutes an inhomogeneous magnetic barrier for charge transport within the 2DEG. The magnetic barriers induced by the FM stripe are shown in figure 1(b). Following [12], the barriers can be approximated as a double delta function, say  $B_z = B \delta(|x| - L/2)$  in our system. A gate voltage is applied on the top of the FM stripe and adjusts the interfacial electric field  $E_z$  and thus Rashba coupling in the 2DEG region beneath the stripe [1]. At both ends of the 2DEG heterostructure are non-magnetic metal contacts that allow the electric current flow through the 2DEG.

In the absence of a magnetic field, the spin degeneracy of the 2DEG energy bands at  $k \neq 0$  is lifted by the coupling of the electron spin with its orbital motion, i.e. spin-orbit coupling. This mechanism is known as the Rashba effect [13]. We consider an electron moving along the  $x$  direction between the two contacts in figure 1(a). Applying the single-particle effective mass approximation, the Hamiltonian of the system can be written as [14]

$$H = \vec{H}_0 + \vec{H}_{SO} = -\frac{\hbar^2 \vec{\nabla}^2}{2m^*} + \frac{eg^*}{2m^*} \frac{\hbar}{2} \vec{B} \cdot \vec{\sigma} + \alpha(-i\vec{\nabla} \times \vec{E}) \cdot \vec{\sigma}. \quad (1)$$

Here  $\vec{H}_0$  is the electronic kinetic energy in the absence of the Rashba effect, while  $\vec{H}_{SO}$  is the Rashba spin-orbit term.  $m^*$  and  $g^*$  are the effective mass and effective Landé factor of the electron, respectively,  $\alpha$  the effective mass parameter and  $\vec{\sigma} = (\sigma_x, \sigma_y, \sigma_z)$  the vector of Pauli

spin matrices.  $\vec{E}$  is the confining electric field in the 2DEG while  $\vec{B}$  is the inhomogeneous magnetic field. For our system,  $\vec{E} = (0, 0, E_z)$  and  $\vec{B} = (0, 0, B_z)$ . Thus in Cartesian coordinates the Hamiltonian reads

$$H = -\frac{\hbar^2}{2m^*} \left( \frac{\partial^2}{\partial x^2} + \frac{\partial^2}{\partial y^2} \right) + \frac{eg^*}{2m^*} \frac{\hbar}{2} B_z \cdot \sigma_z + i \langle \alpha E_z \rangle \left( \sigma_y \frac{\partial}{\partial x} - \sigma_x \frac{\partial}{\partial y} \right) \\ = \begin{pmatrix} \frac{\hbar^2}{2m^*} k_x^2 + \frac{eg^*}{2m^*} \frac{\hbar}{2} B_z + \frac{\hbar^2}{2m^*} [k_y + \frac{e}{\hbar} A_y(x)]^2 & \langle \alpha E_z \rangle \{ik_x + [k_y + \frac{e}{\hbar} A_y(x)]\} \\ -\langle \alpha E_z \rangle \{ik_x - [k_y + \frac{e}{\hbar} A_y(x)]\} & -\frac{\hbar^2}{2m^*} k_x^2 - \frac{eg^*}{2m^*} \frac{\hbar}{2} B_z + \frac{\hbar^2}{2m^*} [k_y + \frac{e}{\hbar} A_y(x)]^2 \end{pmatrix}. \quad (2)$$

Here  $\langle \alpha E_z \rangle$  can be regarded as the spin-orbit coupling parameter (i.e. Rashba parameter), which is proportional to the external electric field for a particular 2DEG.  $A_y(x)$  is the vector potential, which for the double-delta-function magnetic field can be written [15] as  $A_y(x) = B \Theta(L/2 - |x|)$ .  $k_x$  and  $k_y$  are the electron wavevectors along the  $x$  and  $y$  directions. To express all relevant quantities in dimensionless units, we introduce two characteristic parameters: the frequency  $\omega_c = eB_0/m^*$  where  $B_0$  is some typical magnetic field and the length  $l_B = \sqrt{\hbar/eB_0}$ , so that magnetic field  $B(x) \rightarrow B_0 B(x)$ , vector potential  $A(x) \rightarrow B_0 l_B A(x)$ , coordinate  $x \rightarrow l_B x$ , energy  $E \rightarrow \hbar \omega_c E = E_0 E$  and spin-orbit coupling  $\langle \alpha E_z \rangle \rightarrow E_0 l_B \langle \alpha E_z \rangle$ . In reduced units [13], equation (2) can be simplified as

$$H = \begin{pmatrix} H_0^\uparrow & H_{SO}^\uparrow \\ H_{SO}^\downarrow & H_0^\downarrow \end{pmatrix}, \quad (2a)$$

where  $H_0^{\uparrow(\downarrow)} = \frac{1}{2} [k_x^2 + (k_y + A_y(x))^2] \pm \frac{g^* B_z}{4}$  and  $H_{SO}^{\uparrow(\downarrow)} = \langle \alpha E_z \rangle (\pm ik_x + k_y + A_y(x))$ . Because the system is assumed to be unconstrained along the  $y$  direction, the two-dimensional wavefunction  $\Psi(x, y)$  can be written as  $e^{ik_y y} \psi(x)$ .  $\psi(x)$  satisfies the one-dimensional Schrödinger equation

$$H \begin{pmatrix} \psi | \uparrow \rangle \\ \psi | \downarrow \rangle \end{pmatrix} = E \begin{pmatrix} \psi | \uparrow \rangle \\ \psi | \downarrow \rangle \end{pmatrix}, \quad (3)$$

where  $\psi | \uparrow \rangle$  and  $\psi | \downarrow \rangle$  are the wavefunctions for spin-up and down electrons, respectively.

In regions I and III of figure 1(b), there is no spin-orbit effect, so that the Hamiltonian reduces to

$$H = \begin{pmatrix} H_0^\uparrow & 0 \\ 0 & H_0^\downarrow \end{pmatrix}. \quad (4)$$

Let the incident current from the left-hand contact of the device be spin unpolarized and  $E_i$  be the energy of an incident electron with spin up or down. Hence

$$H_0^\uparrow = \langle \uparrow | H | \uparrow \rangle = E_i \\ H_0^\downarrow = \langle \downarrow | H | \downarrow \rangle = E_i. \quad (5)$$

The wavefunction spinor of the electrons in region I is

$$\begin{pmatrix} \psi | \uparrow \rangle \\ \psi | \downarrow \rangle \end{pmatrix} = \begin{pmatrix} a_1 e^{ik_0 x} + b_1 e^{-ik_0 x} \\ c_1 e^{ik_0 x} + d_1 e^{-ik_0 x} \end{pmatrix}, \quad (6)$$

where  $k_0 = \sqrt{2E_i - k_y^2}$  and  $a_1, b_1, c_1$  and  $d_1$  are arbitrary constants. For spin-unpolarized incident current, one simply assumes  $a_1 = c_1 = 1/2$ . Because there is no backward wave in region III, the wavefunctions of the electrons in region III are described by

$$\begin{pmatrix} \psi | \uparrow \rangle \\ \psi | \downarrow \rangle \end{pmatrix} = \begin{pmatrix} a_3 e^{ik_0 x} \\ c_3 e^{ik_0 x} \end{pmatrix}, \quad (7)$$

where  $a_3$  and  $c_3$  are arbitrary constants.

In region II, the presence of the Rashba Hamiltonian will induce a spin-precession effect. The corresponding Schrödinger equation is

$$\begin{pmatrix} E_i - E & H_{SO}^\uparrow \\ H_{SO}^\downarrow & E_i - E \end{pmatrix} \begin{pmatrix} \psi|\uparrow\rangle \\ \psi|\downarrow\rangle \end{pmatrix} = 0, \quad (8)$$

which yields two eigenvalues:

$$\begin{aligned} E_1 &= E_i + \langle \alpha E_z \rangle \sqrt{k_x^2 + (k_y + B)^2} \\ E_2 &= E_i - \langle \alpha E_z \rangle \sqrt{k_x^2 + (k_y + B)^2}. \end{aligned} \quad (9)$$

Corresponding to  $E_1$  and  $E_2$ , one obtains the two eigenvectors, say  $\begin{pmatrix} 1 \\ \alpha_1 \end{pmatrix}$  and  $\begin{pmatrix} 1 \\ \alpha_2 \end{pmatrix}$ , where

$$\alpha_1 = -\alpha_2 = \frac{\sqrt{k_x^2 + (k_y + B)^2}}{ik_x + k_y + B}. \quad (10)$$

Following elaborate examples, now, the relationship between the  $x$  and  $y$  wavevectors in the presence of a  $\delta$ -function  $B$  field has been shown to be [16]  $k_x = \sqrt{2E_i - (k_y + B)^2}$ . Thus the wavefunction spinor in region II is

$$\begin{pmatrix} \psi|\uparrow\rangle \\ \psi|\downarrow\rangle \end{pmatrix} = (a_2 e^{ik_1 x} + b_2 e^{-ik_1 x}) \begin{pmatrix} 1 \\ \alpha_1 \end{pmatrix} + (c_2 e^{ik_2 x} + d_2 e^{-ik_2 x}) \begin{pmatrix} 1 \\ \alpha_2 \end{pmatrix}. \quad (11)$$

Here  $a_2, b_2, c_2, d_2$  are arbitrary constants.  $k_1 = \sqrt{2E_1 - (k_y + B)^2}$  and  $k_2 = \sqrt{2E_2 - (k_y + B)^2}$ .

The eight variables  $b_1, d_1, a_2, b_2, c_2, d_2, a_3$  and  $c_3$  can be found by applying the (i) continuity of wavefunctions, and (ii) step change in the derivative (due to the  $\delta$ -function  $B$  field) at boundaries I–II and II–III for both spin-up and down electrons. The transmission probability for spin-up and down electrons through the device is then calculated as

$$T_\uparrow(E_i, k_y) = \left| \frac{a_3}{a_1} \right|^2 = |2a_3|^2; \quad T_\downarrow(E_i, k_y) = \left| \frac{c_3}{c_1} \right|^2 = |2c_3|^2. \quad (12)$$

The spin polarization ( $P$ ) in the system is then defined as

$$P = \frac{T_\uparrow(E_i, k_y) - T_\downarrow(E_i, k_y)}{T_\uparrow(E_i, k_y) + T_\downarrow(E_i, k_y)}. \quad (13)$$

As reported in [12], the conductance of a tunnelling structure can be calculated in the ballistic regime as the average electron flow over half the Fermi surface, i.e. electrons tunnelling in the possible  $x$  direction. Thus we calculate the conductance for the spin-up ( $G_\uparrow$ ) and spin-down ( $G_\downarrow$ ) electrons in the system by

$$G_{\uparrow(\downarrow)} = G_0 \int_{-\pi/2}^{\pi/2} T_{\uparrow(\downarrow)}(E_F, \sqrt{2E_F} \sin \phi) \cos \phi \, d\phi \quad (14)$$

where  $\phi$  is the incident angle relative to the  $x$  direction and  $E_F$  is the Fermi energy.  $G_0 = e^2 m^* v_F l / \hbar^2$  with  $l$  being the length of the structure in the  $y$  direction and  $v_F$  the Fermi velocity.

In our numerical calculation, a typical InAs system [17] is considered as the 2DEG material for which  $m^* = 0.024 m_0$ ,  $g^* = 15$  and the electron density  $n_e \approx 10^{12} \text{ cm}^{-2}$ . With  $B_0 = 0.5 \text{ T}$ , one has the free-electron Fermi energy of  $E_F \approx 99.54 \text{ meV}$ , and the reduced units  $l_B = 362.7 \text{ \AA}$  and  $E_0 = \hbar \omega_c = 2.37 \text{ meV}$ .

Figure 2 shows the energy dependence of the transmission probability for spin-up ( $T_\uparrow$ ) and spin-down ( $T_\downarrow$ ) electrons while  $\langle \alpha E_z \rangle = 0, 0.1, 0.5$  and  $1$ , respectively. When  $\langle \alpha E_z \rangle = 0$ ,

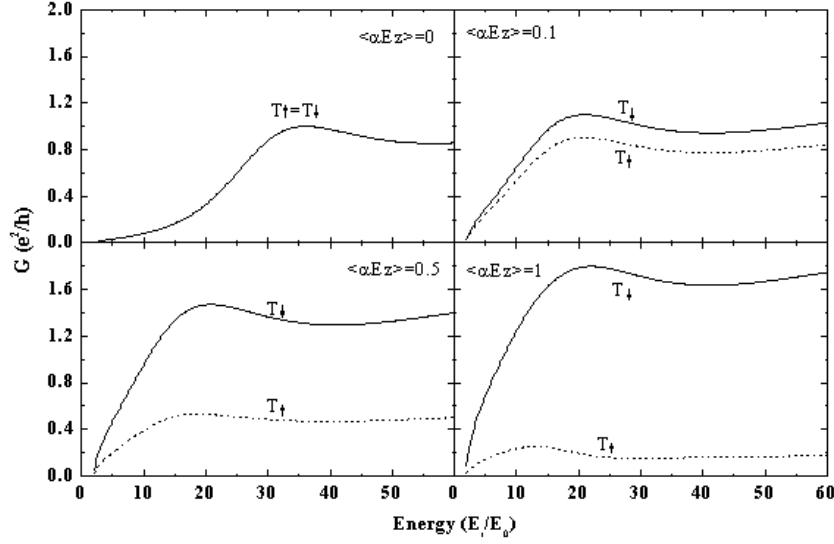


**Figure 2.** The transmission probability of spin-up ( $T_\uparrow$ ) and spin-down ( $T_\downarrow$ ) electrons as a function of incident energy when  $\langle \alpha E_z \rangle = 0, 0.1, 0.5$  and  $1$ , where  $k_y = 2$ ,  $g^* = 15$ ,  $L = 0.5$  and  $B = 0.5$ .

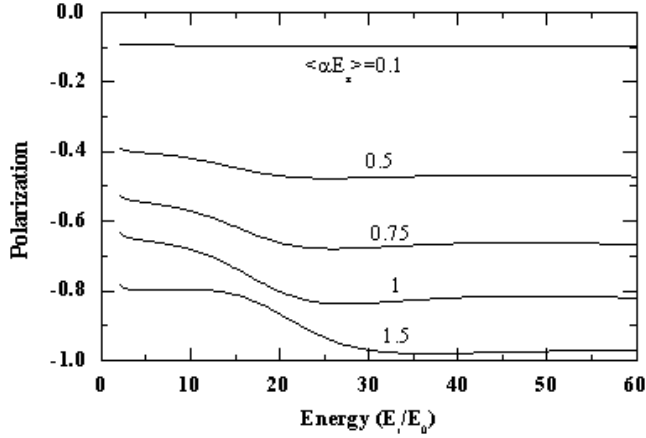


**Figure 3.** The energy dependence of spin polarization  $P$  under different  $\langle \alpha E_z \rangle$ , where  $k_y = 2$ ,  $g^* = 15$ ,  $L = 0.5$  and  $B = 0.5$ .

there is no difference between the transmission probability of spin-up and spin-down electrons, which means no spin polarization in the system. This is expected because the  $B_z(x)$  is anti-symmetric and thus any differential effect on the up/down spin caused by the positive  $B$ -field will be compensated by the opposite effect induced by the negative  $B$ -field in the absence of the Rashba effect. In the presence of non-zero  $\langle \alpha E_z \rangle$ , there exists a mixing of spin-up and down electrons since the eigenfunctions in region II consist of both spin-up and down components. The different degree of spin mixing for spin-up and down electrons eliminates the antisymmetry of the system and results in a difference between  $T_\uparrow$  and  $T_\downarrow$ , i.e. the spin injection in the system. The energy dependence of spin polarization under different Rashba parameters ( $\langle \alpha E_z \rangle$ ) is given in figure 3. The spin polarization increases monotonically with the Rashba parameter ( $\langle \alpha E_z \rangle$ )

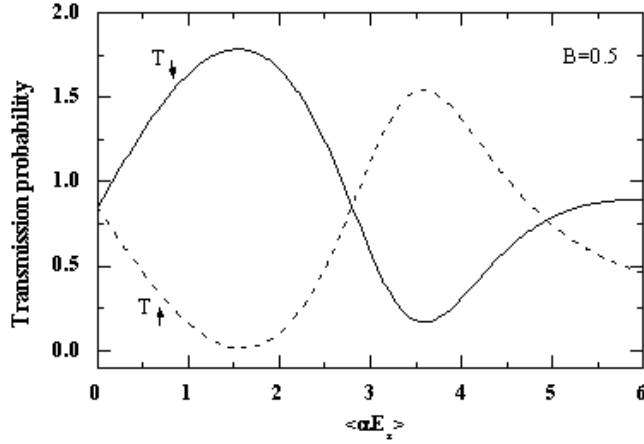


**Figure 4.** The transmission probability of spin-up and down electrons as a function of Rashba coupling  $\langle \alpha E_z \rangle$ , where  $k_y = 2$ ,  $g^* = 15$ ,  $L = 0.5$ ,  $B = 0.5$  and  $E_i = E_F = 42$ .

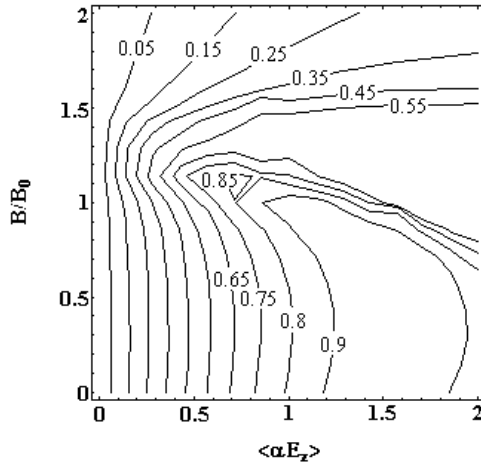


**Figure 5.** Contour plot of the spin polarization ( $P$ ) as a function of magnetic field and Rashba coupling  $\langle \alpha E_z \rangle$ , where  $k_y = 2$ ,  $g^* = 15$ ,  $L = 0.5$  and  $E_i = E_F = 42$ .

and reaches  $\sim 95\%$  at  $\langle \alpha E_z \rangle \approx 1.5$ . Note that the experimentally obtained intrinsic spin-orbit coupling constant in 2DEG in the absence of external electric field is around  $10^{-11}$  eV m, which means that it should not be difficult to get  $\langle \alpha E_z \rangle = 1.5 \approx 8.58 \times 10^{-11}$  eV m by applying an external electric field. We fix the energy of the incident electrons to the Fermi energy, i.e.  $E_i = E_F = 99.54/2.37$  meV  $\approx 42$ , and calculate the  $T_{\uparrow}$  and  $T_{\downarrow}$  as a function of  $\langle \alpha E_z \rangle$ , as shown in figure 4. For the incident electrons with Fermi energy,  $T_{\uparrow}$  is the same as  $T_{\downarrow}$  when  $\langle \alpha E_z \rangle = 0$ . With increasing  $\langle \alpha E_z \rangle$ ,  $T_{\uparrow}$  and  $T_{\downarrow}$  oscillate in value, thus showing clearly that the spin-conductance modulation in the system, and thus the spin polarization in the proposed structure, obviously arises from the spin precession induced by the Rashba effect. Additionally, the oscillations in  $T_{\uparrow}$  and  $T_{\downarrow}$  are anti-phase to each other, resulting in a large spin-polarization maximum in the middle of each cycle.

Figure 5 gives a contour plot of the magnetic field and Rashba coupling dependence of spin polarization ( $-P$ ) for the incident electrons with Fermi energy. What is noteworthy is

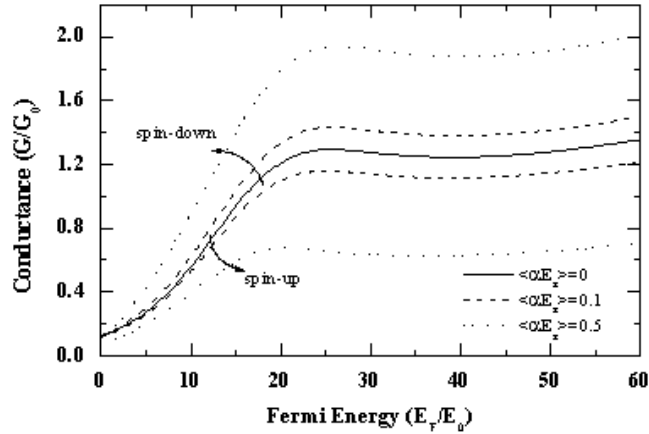


**Figure 6.** The conductance under different Rashba couplings for spin-up ( $G_{\uparrow}$ ) and spin-down ( $G_{\downarrow}$ ) electrons as a function of Fermi energy.

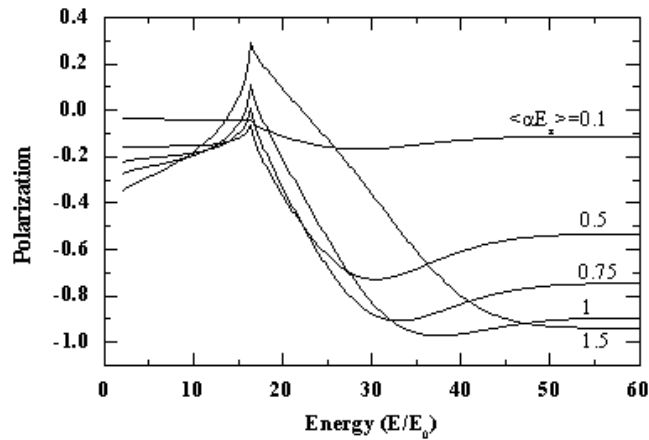


**Figure 7.** The energy dependence of spin polarization  $P$  under different  $\langle \alpha E_x \rangle$  while the magnetization of the FM stripe is switched towards the  $x$ -axis direction, where  $k_y = 2$ ,  $g^* = 15$ ,  $L = 0.5$  and  $B = 0.5$ .

that the strength of the magnetic fringe field can be used to tune the spin-polarization ratio to its maximum possible value although the magnetic field on its own cannot induce any spin polarization without Rashba coupling. For instance,  $P$  exceeding 0.9 can be achieved at  $\langle \alpha E_x \rangle$  of less than unity if a unit  $B$  field is applied, whereas a higher  $\langle \alpha E_x \rangle$  is required in the absence of  $B$  field. This maybe useful in a practical system, as too large an applied electric field may affect the integrity of the 2DEG.

The conductance under different Rashba couplings for spin-up and down electrons normalized by  $G_0$  is also calculated as a function of Fermi energy, which can be adjusted by changing the carrier density of the 2DEG, as shown in figure 6. Along with the increase of Rashba coupling, the conductance of spin-up electrons decreases while that of spin-down electrons increases, which also demonstrates the spin precession in our system.

It is not only the magnitude but also the direction of magnetic field that can affect the spin injection in the structure. When we switch the magnetization of the FM stripe towards the



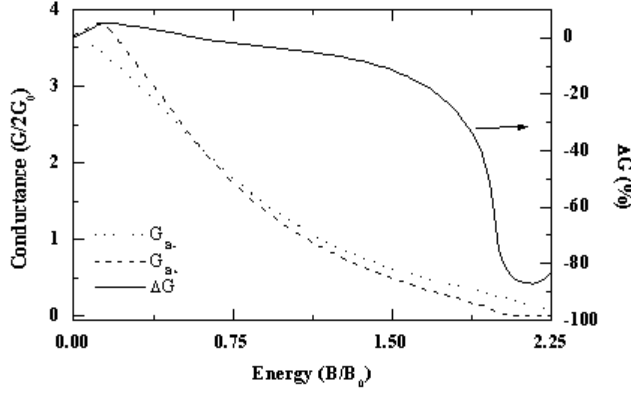


**Figure 8.** The magnetic field dependence of the conductance  $G_{B+}$ ,  $G_{B-}$  and  $\Delta G$ , where  $L = 0.5$ ,  $g^* = 15$  and  $E_i = E_F = 42$  and  $\langle \alpha E_z \rangle = 1$ .

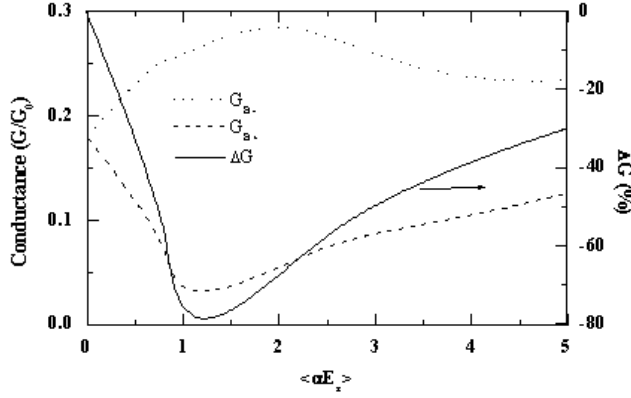


**Figure 9.** The Rashba coupling dependence of the conductance  $G_{B+}$ ,  $G_{B-}$  and  $\Delta G$ , where  $B = 2$ ,  $L = 0.5$ ,  $g^* = 15$  and  $E_i = E_F = 42$ .

$x$ -axis direction, the inhomogeneous magnetic fields will change into that shown in figure 1(c). In this case, the spin polarization as a function of incident electron's energy is given in figure 7. Comparing figure 7 with 3, the switching of magnetization of the FM stripe greatly affects the spin polarization in the system, especially for the electrons with lower energy.

It is noteworthy that the conductance of the proposed structure also changes with the switching of the magnetization direction of the FM stripe and thus the structure exhibits MC behaviour. The conductance of the structure is defined as  $G = G_{\uparrow} + G_{\downarrow}$ . We use  $G_{B\pm}$  to represent the conductance while the magnetization of the FM stripe points to the  $\pm x$ -axis directions. Then the MC ratio ( $\Delta G$ ) is defined by

$$\Delta G = \frac{G_{B+} - G_{B-}}{G_{B+} + G_{B-}} \times 100\%. \quad (15)$$

Figure 8 plots the magnetic field dependence of the conductance  $G_{B+}$ ,  $G_{B-}$  and  $\Delta G$ . The negative MC increases with increasing magnetic field and reaches  $\sim 90\%$  at a relatively low optimum value of  $\langle \alpha E_z \rangle \sim 1$ . Such a large MC ratio compares favourably with conventional spin-valve devices, and suggests the potential of using the structure in new generation magnetic sensors. The MC is also greatly affected by the strength of the Rashba coupling (and thus the external electric field), as shown in figure 9.

In summary, we have calculated the spin dependent transport properties of an FM/2DEG structure in the presence of the Rashba effect. The gate electrode on top of the device can be used to modulate the Rashba coupling and thus the spin injection in the 2DEG. The combination of Rashba coupling and fringe field effects enables the structure to achieve a high degree of spin polarization and high MC ratio, thus opening the way for its application in spin-logic and magnetic sensor applications, respectively.

## References

- [1] Datta S and Das B 1990 *Appl. Phys. Lett.* **56** 665
- [2] Bychkov Y A and Rashba E I 1984 *J. Phys. C: Solid State Phys.* **17** 6039
- [3] Rashba E I 2000 *Phys. Rev. B* **62** 16267
- [4] Kikkawa J M and Awschalom D D 1998 *Phys. Rev. Lett.* **80** 4313
- [5] Nitta J *et al* 1997 *Phys. Rev. Lett.* **78** 1335
- [6] Monzon F G and Roukes M 1999 *J. Magn. Magn. Mater.* **198/199** 632  
Gardelis S, Smith C G, Barnes C H W, Linfield E H and Ritchie D A 1999 *Phys. Rev. B* **60** 7764
- [7] Labella V 2001 *Science* **292** 1518  
Heersche H B, Schäpers Th, Nitta J and Takayanagi H 2001 *Phys. Rev. B* **64** R161307
- [8] Grundler D 2001 *Phys. Rev. B* **63** R161307  
Hu C-M and Matsuyama T 2001 *Phys. Rev. Lett.* **87** 066803
- [9] Wolf S A, Awschalom D D, Buhrman R A, Daughton J M, von Molnár S, Roukes M L, Chtchelkanova A Y and Treger D M 2001 *Science* **294** 1488
- [10] Schmidt G, Ferrand D, Molenkamp L W, Filip A T and van Wees B J 2000 *Phys. Rev. B* **62** R4790
- [11] Fiederling R *et al* 1999 *Nature* **402** 787  
Ohno Y *et al* 1999 *Nature* **402** 790
- [12] Majumdar A 1996 *Phys. Rev. B* **54** 11911
- [13] Mireles F and Kirczenow G 2001 *Phys. Rev. B* **64** 024426
- [14] Molenkamp L W, Schmidt G and Bauer G E W 2001 *Phys. Rev. B* **64** 121202
- [15] Peeters F M and Matulis A 1993 *Phys. Rev. B* **48** 15–166
- [16] Xu H Z and Okada Y 2001 *Appl. Phys. Lett.* **79** 3119
- [17] Papp G and Peeters F M 2001 *Appl. Phys. Lett.* **78** 2184